ZnO Thin Films Synthesized by Sol–Gel Process for Photonic Applications

L. Znaidi[a,*], T. Touam[b], D. Vrel[a], N. Souded[a], S. Ben Yahia[a], O. Brinza[a], A. Fischer[b] and A. Boudrioua[b]

[a]Laboratoire des Sciences des Procédés et des Matériaux, CNRS/UPR 3407, Université Paris 13

99 Av. J.-B. Clément, 93430 Villetaneuse, France

[b]Laboratoire de Physique des Lasers, CNRS/UMR 7538, Université Paris 13

99 Av. J.-B. Clément, 93430 Villetaneuse, France

Undoped and aluminum-doped ZnO thin films are prepared by the sol–gel process. Zinc acetate dihydrate, ethanol and monoethanolamine are used as precursor, solvent and stabilizer, respectively. In the case of Al-doped ZnO, aluminum nitrate nonahydrate is added to the precursor solution with an atomic percentage equal to 1 or 2 at.% Al. The multi thin layers are prepared by spin-coating onto glass substrates, and are transformed into ZnO upon annealing at 550 °C. Films with preferential orientation along the *c*-axis are successfully obtained. The structural, morphological, and optical properties of the thin films as a function of aluminum content have been investigated for different elaboration parameters (e.g. layer number) using X-ray diffraction, atomic force microscopy, scanning electronic microscopy. Waveguiding properties of the thin films have been also studied using *m*-lines spectroscopy. The results indicate that our films are monomodes at 632.8 nm with propagation optical loss estimated around 1.6 dB/cm.

1. Introduction

Zinc oxide (ZnO) is an emerging material for a large number of areas. Unlike many of its competitors, ZnO is inexpensive, relatively abundant, chemically stable, easy to prepare, non toxic and most of the doping materials that are used with it are also readily available. It has been used in a variety of applications such as conductive films, solar cell windows, photoelectric cells, nonlinear optics, bulk and surface acoustic wave devices [1–3], and micro mechanic devices [4, 5]. ZnO wide band gap opens the possibility of creating ultraviolet (UV) light emission diodes (LEDs) and white LEDs with superior color purity. Furthermore because of its transparency and its electro-optical and elasto-optical properties, ZnO is attractive for integrated photonic devices.

ZnO thin films have been made by a variety of techniques, among which there can be mentioned reactive sputtering [6], spray pyrolysis [7], zinc oxidation [8], electro deposition [9], pulsed laser deposition [10], chemical vapor deposition (CVD) [11], metalorganic CVD (MOCVD) [12], plasma enhanced CVD (PECVD) [13], low pressure sputtering [14], chemical bath deposition (CBD) [15], and sol–gel route [16]. The sol–gel method has emerged as one of the most promising processing route as it is particularly efficient in producing thin, transparent, homogeneous, multi component oxide films of many compositions on various substrates at low cost

and it allows the tuning of the refractive index and thickness of the film by varying synthesis parameters.

In this work, we have investigated the structural, morphological, and optical properties of undoped and Al-doped ZnO thin film spin-coated on glass substrates. We report guided modes spectra for both transverse electric (TE) and transverse magnetic (TM) polarization in undoped and Al-doped ZnO waveguides. From angular spectra modes, we have measured effective indices which permit to determine ordinary and extraordinary refractive indices of the thin films. Propagation losses of the thin films have been also carried out.

2. Experimental

ZnO thin films were prepared by the sol–gel process [16]. As a starting material, zinc acetate dihydrate ($Zn(CH_3COO)_2 \cdot 2H_2O$) was dissolved in a mixture of ethanol and monoethanolamine (MEA) solution with a concentration of 0.75 mol L^{-1}. MEA acts at the same time as a base and a complexing agent and the MEA to zinc acetate molar ratio was fixed at 2. For doped films, aluminum nitrate nonahydrate ($Al(NO_3)_3 \cdot 9H_2O$) was added to the mixture with an atomic percentage fixed at 1 or 2 at.% Al. The precursor solution was deposited on glass substrates by spin-coating (3000 rpm, 30 s). As synthesized films, doped and undoped, were preheated at 300 °C for 10 min after each coating. This procedure was repeated up to nine times to increase the thickness. The films were subsequently heated up to 550 °C for 2 h in order to obtain crystallized ZnO.

———————
* corresponding author; e-mail: `lamia.znaidi@lspm.cnrs.fr`

The samples were characterized by X-ray diffraction (XRD) using an Inel G3000 diffractometer, with a copper anode, monochromated using a Ge single crystal monochromator (Cu K_{α_1}: 1.54056 Å). Incident angle ω was equal to 1°, and detection angles were ranging from $2\theta = 20$ to 110° using a curved detector having a 50 cm radius and a 90° aperture. Scanning electronic microscopy (SEM) was performed using a Leica S440 microscope, atomic force microscopy (AFM) by a Veeco Nanoscope DIM3, and *m*-lines spectroscopy [17].

3. Microstructural characterizations

Figure 1 presents the AFM images of the ZnO surfaces. From these images, the roughness mean square (RMS) value can be extracted and seems to be significantly dependent on the Al content: an undoped single layer sample would present an RMS of 6.44 nm, whereas a 2 at.% Al sample would present an RMS value of 17.08 nm. Inversely, the roughness does not evolve significantly with the number of layers: an undoped sample displays an RMS = 6.44 nm for the single layer sample, to an RMS of 9.68 nm for the 9-layer sample.
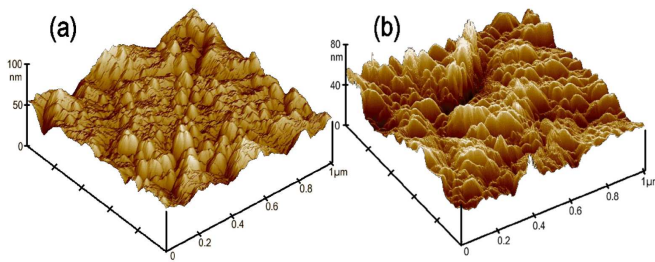

Fig. 1.   AFM images of 5-layer ZnO films: undoped ZnO (a), and 2 at.% Al doped ZnO (b).

Figure 2 represents the diffraction pattern for an undoped 5-layer sample. The pattern clearly shows an over-expression of the (002) peak, and an under-expression of every other peak, except for the (103) peak.
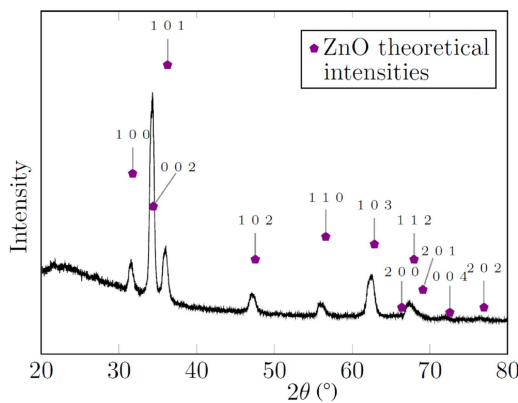

Fig. 2.   X-ray diffraction pattern of a 5-layer, undoped sample.   Marks represent the theoretical intensities of the peaks for a randomly oriented ZnO.

To quantify this preferential orientation, texture coefficients (TC) were calculated using the relative intensities of randomly oriented ZnO given in the 36-1451 JCPDS card for the 7 most intense reflections, (100), (002), (101), (102), (110), (103), and (112) peaks, according to the method described by Barret and Massalski [18]. From this analysis, the sample displays a strong (002) and a slight (103) texture. It seems that this phenomenon gets stronger with the number of layers; however, for Al-doped ZnO, if the texture is still strong, it does not evolve the number of layers.
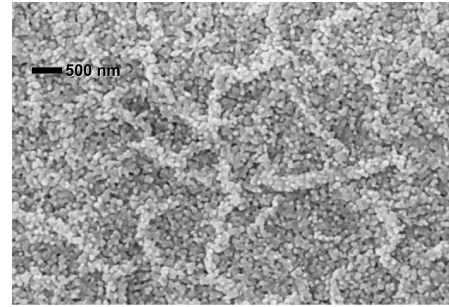

Fig. 3.   Scanning electronic micrograph of a 5-layer undoped sample (magnification ×50,000).

Figure 3 represents the SEM observation of the same sample, i.e. undoped, 5-layer ZnO film. The film can be described as a structure of very fine particles, around 100 nm, but this structure is not completely flat and looks wrinkled. When a similar observation is performed on a doped sample, the flatness of the film is greatly increased, and thus, using doped ZnO may improve the waveguiding properties, which are directly dependent on the roughness.

4. Optical characterizations

To investigate the waveguide optical properties of pure and aluminum doped ZnO thin films, we used dark *m*-lines spectroscopy [17]. This technique uses a prism coupling method. Besides, the waveguiding properties of the film strongly depend on the microstructure of the material: surface roughness, porosity and grain size which are connected to the fabrication process parameters such as spin speed, sol concentration, treatment temperature and number of coating layers. The mode profiles in both the TE and TM polarizations are obtained by measuring the reflected intensity of a (He–Ne at 632.8 nm) laser beam, as a function of the incidence angle. The measurements were carried out on the film deposited on glass substrate. Figure 4 shows the typical TE and TM guided modes spectra of 9-layer, undoped and Al-doped ZnO films. The results show that our thin films support only the fundamental TE_0 and TM_0 modes.

From the angular position of the reflectivity dips we compute the effective mode indices. These last ones serve to calculate the refractive indices and the thickness of the
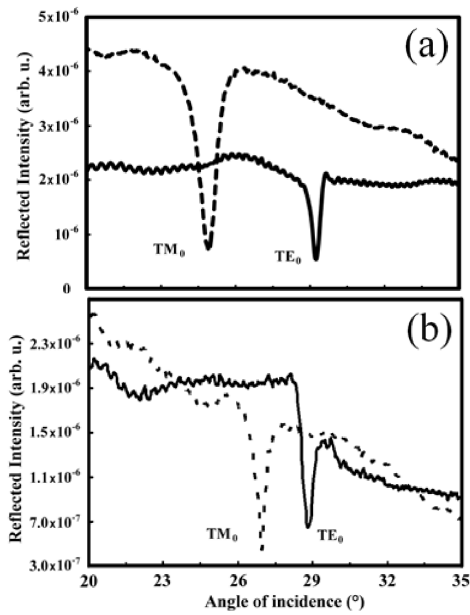
Fig. 4. Typical TE and TM guided mode spectra of: (a) undoped ZnO, (b) 1 at.% Al doped ZnO.
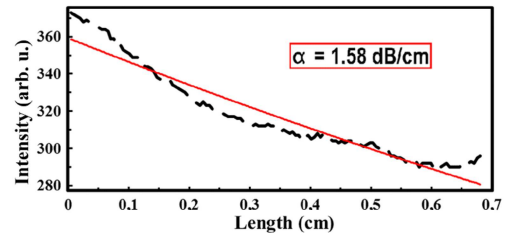

Fig. 5. Optical attenuation of the fundamental TE mode in 7-layer undoped ZnO thin film. Surface scattering loss measurement, with exponential fit (in red).

is calculated in dB/cm. The overall loss measured is the combined total of both scattering loss from particles or other scattering centers and surface roughness, and the inherent absorption of the waveguide material. The optical losses have been estimated to be $\alpha = 1.6$ dB/cm.

5. Conclusion

In this work we reported the investigation of pure and Al doped ZnO thin films prepared by sol–gel method for optical waveguiding applications. The prepared samples display a very strong (0 0 2) preferential orientation. SEM and AFM characterizations have been focused on roughness (RMS), which is known to be strongly correlated to the optical losses, and surface morphologies have shown that the quality of the films synthesized is well adapted to the considered application. The optical properties determined by *m*-lines spectroscopy are promising for further waveguiding application. All the films are displaying well guided modes meaning that the coupling and confinement of the light in the film is efficient. The optical loss was estimated to be around 1.6 dB/cm, using the moving fiber method. Therefore, the sol–gel method was proved to be well adapted to the elaboration of thin films for photonic applications.

film. These parameters are related to the effective mode indices [17]. At least two modes are generally needed. Because our waveguides are single mode, we use the measured value of the effective indices and that of thickness measured by the SEM. The calculation is based on the least squares method widely discussed by Kersten [19] and the results are reported in Table.

TABLE

Measured fundamental TE and TM effective indices, refractive indices and thickness of the undoped and 1 at.% Al doped ZnO 9-layer films.

	Undoped ZnO		1 at.% Al doped ZnO	
	TE	TM	TE	TM
effective index, N_0	1.7181	1.5690	1.7258	1.5450
thickness [nm], d	479		450	
refractive index, n	1.7837		1.7978	

The results show that doping ZnO with 1 at.% Al leads to increase of the refractive index for both TE and TM polarizations. We also noted that the guided modes are better confined.

The determination of optical attenuation in waveguides is of great interest for designing integrated optical devices. Several techniques can be used for loss measurement. In our case, we have used the prism-in coupling and the moving fiber method (Metricon Model 2010) in which the exponential decay of light is measured by a fiber probe scanning down the length of the propagation streak. The result of the optical attenuation measured in a 7-layer undoped ZnO film is depicted in Fig. 5.

A least squares exponential fit is then made to the intensity as a function of distance patterns and the loss

References

[1] T.L. Yang, D.H. Zhang, J. Ma, H.L. Ma, Y. Chen, *Thin Solid Films* **326**, 60 (1998).

[2] M. Tomar, V. Gupta, K. Sreenivas, A. Mansingh, *Dev. Mater. Reliabil.* **5**, 494 (2005).

[3] T. Mitsuyu, O. Yamazaki, K. Ohji, K. Wasa, *Ferroelectrics* **42**, 233 (1982).

[4] F.R. Blom, D.J. Yntema, F.C.M. Van de Pol, M. Elwenspoek, J.H.J. Fluitman, Th.J.A. Popma, *Sensors Actuators* **A21-A23**, 226 (1990).

[5] C.J. Van Mullem, F.R. Blom, J.H.J. Fluitman, M. Elwenspoek, *Sensors Actuators* **A25-27**, 379 (1991).

[6] Z. Li, W. Gao, *Mater. Lett.* **58**, 1363 (2004).

[7] J.H. Lee, B.W. Yeo, B.O. Park, *Thin Solid Films* **457**, 333 (2004).

[8] H. Kashani, *J. Electron. Mater.* **27**, 876 (1998).

[9] P. Souletie, S. Bethke, B.W. Wessels, H. Pan, *J. Cryst. Growth* **86**, 248 (1988).

[10] G.I. Petrov, V. Shcheslavskiy, V.V. Yakovlev, I. Ozerov, E. Chelnokov, W. Marine, *Appl. Phys. Lett.* **83**, 3993 (2003).

[11] X.T. Zhang, Y.C. Liu, J.Y. Zhang, Y.M. Lu, D.Z. Shen, X.W. Fan, X.G. Kong, *J. Cryst. Growth* **254**, 80 (2003).

[12] B. Sang, Y. Nagoya, K. Kushiya, O. Yamase, *Sol. Energy Mater. Sol. Cells* **75**, 179 (2003).

[13] B.S. Li, Y.C. Liu, Z.Z. Zhi, D.Z. Shen, Y.M. Lu, J.Y. Zhang, X.G. Kong, X.W. Fan, *Thin Solid Films* **414**, 170 (2002).

[14] Y. Chen, D.M. Bagnall, H. Koh, K. Park, K. Hiraga, Z. Zhu, T. Yao, *J. Appl. Phys.* **84**, 3912 (1998).

[15] M. Ortega-López, A. Avila-García, M.L. Albor--Aguilera, V.M. Sánchez Resendiz, *Mater. Res. Bull.* **38**, 1241 (2003).

[16] L. Znaidi, *Mater. Sci. Eng. B* **174**, 18 (2010).

[17] P.K. Tien, R. Ulrich, *J. Opt. Soc. Am.* **60**, 1325 (1970).

[18] C.S. Barret, T.B. Massalski, *Structure of Metals*, Pergamon Press, Oxford 1980, p. 205.

[19] R.Th. Kersten, *Opt. Commun.* **9**, 427 (1973).